2-2018

A Mean-Risk Mixed Integer Nonlinear Program for Transportation Network Protection

Jie Lu
JD.com

Akshay Gupte
Clemson University, agupte@clemson.edu

Yongxi Huang
Amazon.com, Inc.

Recommended Citation

A Mean-Risk Mixed Integer Nonlinear Program for Transportation Network Protection

Jie Lu[a,1], Akshay Gupte[b,*], Yongxi Huang[c,1]

[a]*Algorithm Design and Development, JD.com*
[b]*Department of Mathematical Sciences, Clemson University*
[c]*Amazon.com, Inc.*

Abstract

This paper focuses on transportation network protection to hedge against extreme events such as earthquakes. Traditional two-stage stochastic programming has been widely adopted to obtain solutions under a risk-neutral preference through the use of expectations in the recourse function. In reality, decision makers hold different risk preferences. We develop a mean-risk two-stage stochastic programming model that allows for greater flexibility in handling risk preferences when allocating limited resources. In particular, the first stage minimizes the retrofitting cost by making strategic retrofit decisions whereas the second stage minimizes the travel cost. The conditional value-at-risk (CVaR) is included as the risk measure for the total system cost. The two-stage model is equivalent to a nonconvex mixed integer nonlinear program (MINLP). To solve this model using the Generalized Benders Decomposition (GBD) method, we derive a convex reformulation of the second-stage problem to overcome algorithmic challenges embedded in the non-convexity, nonlinearity, and non-separability of first- and second- stage variables. The model is used for developing retrofit strategies for networked highway bridges, which is one of the research areas that can significantly benefit from mean-risk models. We first justify the model using a hypothetical nine-node network. Then we evaluate our decomposition algorithm by applying the model to the Sioux Falls network, which is a large-scale benchmark network in the transportation research community. The effects of the chosen risk measure and critical parameters on optimal solutions are empirically explored.

Keywords: Transportation, Retrofitting, CVaR, Stochastic mixed integer nonlinear optimization, Generalized Benders decomposition
2010 MSC: 90B06, 90C11, 90C15, 90C90

[*]Corresponding author
  Email addresses: `jielu1301@outlook.com` (Jie Lu), `agupte@clemson.edu` (Akshay Gupte), `erichuang05@gmail.com` (Yongxi Huang)
  [1]The work was done mostly when the author was at Glenn Department of Civil Engineering, Clemson University

1. Introduction

Many highway bridges in the United States (U.S.), especially old bridges, can be seriously damaged or collapse even in relatively moderate natural disasters, such as mild earthquakes [1]. In a recent infrastructure report card issued by the American Society of Civil Engineers (ASCE), one in nine U.S. bridges was deemed structurally deficient [2]. Since 1960's, major structural damage has caused millions of dollars of economic losses in a number of states, including Alaska, California, Washington, and Oregon [1]. To improve this situation, at-risk bridges must be identified and evaluated and retrofitting programs should be in place to strengthen its resilience [1]. Highway bridge retrofit is one of the most common approaches undertaken by federal and state departments of transportation in order to mitigate negative effects of extreme events on highway transportation networks. Bridge damages due to extreme events may result in direct social and economic losses as a result of post-disaster bridge repair and restoration. There may also be indirect impacts on transportation networks due to short-term evacuations and emergency responses [3], and even long-term changes in travel activities [4, 5]. These adverse impacts can be avoided or alleviated if proactive bridge retrofit strategies are deployed.

The Federal Highway Administration (FHWA) estimates that to eliminate the backlog of all deficient bridges by 2028, an annual investment of $20.5 billion is needed; however, currently only $12.8 billion is being spent [2]. Due to the limited retrofitting resources, it is neither practical nor economical to retrofit all bridges to their full health conditions and thus a prioritized retrofitting scheme is expected. In practice, resources are prioritized to bridges based on ranked structural deficiencies [1] which neglects the effects of networked bridges. The resultant solution may be sub-optimal if indirect social losses (e.g., travel delay cost) are considered, since traffic flows are allowed to redistribute over the transportation network and affect other at-risk bridges. This justifies the need to consider bridge retrofitting strategies at a network level.

1.1. Example of a network-based model

Let us consider the benchmark Sioux Falls network, which is commonly used in the transportation research community (cf. LeBlanc et al. [6]), to better understand the importance of a networked model. Refer to Figure 1. Assume that there are four bridges, labeled as A, B, C, and D, which are vulnerable to seismic hazards.

A failure of bridge C (i.e., functional obsolescence) would detour the traffic on link 60 from node #20 to #18 to a longer path consisting of links 61, 58, 52 and 50. This may result in higher travel cost, due to detours and resulting congestion. Additionally, the varied structural deficiencies of each bridge may require the use of different materials and labor for its rehabilitation. The main challenge is then formulating strategic allocations of limited resources to the bridges before they become structurally inadequate and cause undesirable consequences to the network. A strategy solely based on the ranked structural deficiency status would not guarantee system optimality. For instance, assuming that bridge D is in a worse condition than bridge C and that resources are insufficient to support retrofitting both of them, bridge D will
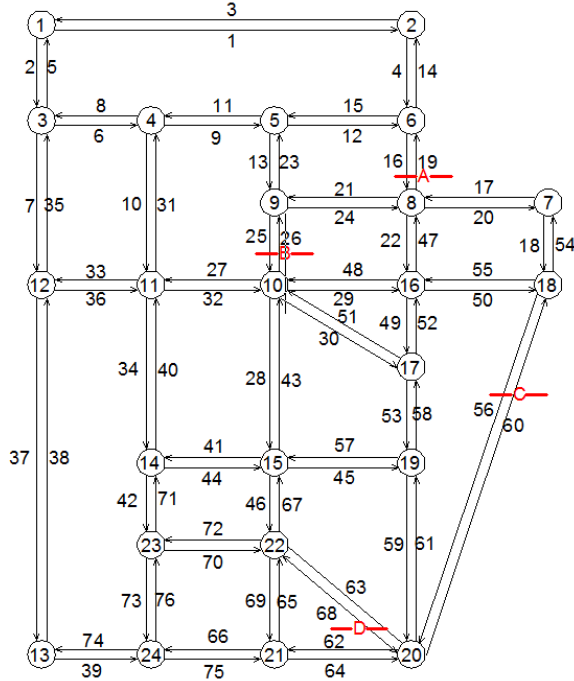
Figure 1: Sioux Falls network

outrank bridge C in retrofit priority, thus possibly exposing bridge C to a higher chance of reaching the state of functional obsolescence in extreme events. This solution could be highly sub-optimal, as the failure of bridge D only affects traffic on links among nodes #20, #21 and #22 while the failure of bridge C affects traffic on links among nodes #20, #19, #17, #16, and #18. From a network perspective, bridge C would be better positioned to be retrofitted.

1.2. Relevant literature

Network-based bridge retrofitting is a general transportation network protection problem, which can be grouped into two broad categories, depending on whether bridges are treated as links [3, 5, 7] or as paths [8, 9]. The former approach formulates as maximum capacity or minimum cost network flow design problems with a focus on long-term economic effect of retrofit, whereas the latter formulates maximal covering network design problems, which are more focused on short-term emergency response or maximal coverage of population centers. From a transportation system analysis viewpoint, the transportation network protection problem is essentially a network design problem (NDP), in which the upper-level problem involves optimal retrofit decisions for best social welfares (e.g., minimum retrofitting cost and travel delay) while the lower-level problem accounts for the behaviors of network users which normally present demand-performance equilibrium [10, 11, 12, 13, 14].

Uncertainty is naturally embedded in almost all transportation protection problems. Engineering methods based on the wait-and-see approach [15] seek optimal solutions upon the realizations of uncertainty (in the form of scenarios), that is, the engineering methods focus on the deterministic optimization problems. The resulting scenario dependent solutions are then aggregated in order to be implemented [3, 16, 17, 18, 19]. However, since future events are unknown at the time of making decisions, scenario-specific solutions (policies) may not even be feasible for other possible scenarios. Thus, a method that can account for a large number of possible scenarios needs to be developed. Previous studies use either stochastic programming (SP) [5, 7, 20] or robust optimization (RO) method [21, 22, 23, 24] to take into account all scenarios. In general, the SP method takes the expectation of consequences of all scenarios and thus is *risk-neutral* and suitable for problems aiming to achieve long-term economic effects; however, it may have poor performance under extreme events. Though rare, these extreme event hazards exert severe impacts on the system. RO approach, on the other hand, considers worst-case scenario with low-occurrence probability, which may lead to too conservative and in most cases costly solutions. Therefore, neither risk-neutral SP approach nor RO-based method is best to capture the variability of risk. This motivates us to seek a new method for economic, yet robust, solutions.

In literature, a balance between risk-neutral SPs and RO is accomplished by incorporating a risk measure into the stochastic program. Such models are referred to as *mean-risk* SPs. The conditional value-at-risk (CVaR) is a commonly used risk measure for this purpose. It was first introduced as a risk assessment technique in portfolio management for hedging a portfolio of financial instruments to reduce risk [25, 26]. Since then, it has been applied to a number of engineering applications, such as electricity operations [27], water resources allocation [28], facility location planning [29], disaster management [30], and hazard material routing [31]. Given a probability distribution and a confidence level α, CVaR is a weighted average of value-at-risk (VaR), which is the lower α-quantile, and the incremental values beyond the VaR cutoff point in the distribution. Thus, CVaR accounts for losses exceeding VaR. Since VaR is monotone in α, a higher confidence level leads to a more risk-averse solution. The RO problem is equivalent to considering a sufficiently large α (worst-case scenario). CVaR has the desirable property of coherence [32, 33], meaning that it is a translation invariant, subadditive, positive homogenous, monotonic function, whereas VaR is a highly nonconvex function [34]. Despite its coherence, CVaR presents some computational challenges in solving mean-risk SPs, and this has motivated numerous algorithmic developments for decomposition methods with cutting-plane approaches [28, 30, 35, 36, 37, 38, 39]. CVaR falls under the category of quantile risk measures, as opposed to being one of the deviation risk measures such as expected excess and absolute semi-deviation [40]. Both types of risks take into account the scenarios that exceed some pre-specified target; the former enjoys the benefit of allowing the user to specify a quantile-level of the underlying distribution as a target whereas the latter either uses the mean as the target value or requires some other scalar value to be specified for the target.

1.3. Contributions of this study

In this study, we adopt CVaR as the risk measure in developing a mean-risk two-stage stochastic programming model for transportation network protection problems, with the goal of minimizing the direct cost of retrofitting bridges in the first stage and indirect travel cost in the second stage. The first-stage decisions indicate the assignments of retrofit strategies to different bridges in an optimized manner, and are made simultaneously with second-stage traffic assignment decisions. CVaR is used to penalize scenarios with large losses using a user-specified confidence level and the risk consequence is integrated with the two-stage stochastic program with a trade-off coefficient. The model is generic and generalizable to different kinds of natural and man-made disasters.

In the context of transportation network protection, the proposed study is, to the best of our knowledge, the first study undertaken with CVaR as the risk measure. Our proposed model is closely related to the stochastic transportation protection model by Liu et al. [5], in which a central semi-deviation risk measure is used. However, our study is distinct from this prior study and advances the models in the following aspects. First, the semi-deviation measure can only capture the effects of scenarios that are worse than the expectation of second stage costs while CVaR is flexible to incorporate a spectrum of scenarios, depending on the pre-defined confidence level and the weight of the risk measure. Second, the prior studies held the assumptions of the binary damage states (i.e., either no damage or collapse) and binary retrofit strategies (i.e., retrofit or no retrofit). Although these assumptions help reduce the problem size and consequently the computational challenges associated with solving large-scale problems, this simplification may result in less informative solutions and overestimate costs. In this study, we relax the assumption by defining multiple damage states and multiple retrofit strategies based on a recent study [41] where binary decision variables are used to indicate whether a specific strategy is selected for a bridge. From the modeling perspective, it is not a trivial extension to the prior efforts due to the inherent correlations between retrofit strategies, damage states, and resulting distributions of traffic flows on the network. In addition, bridge retrofit strategies are subject to a budget limit, thereby adding to the combinatorial complexity of the problem.

The mean-risk two-stage stochastic programming model is formulated as a non-convex mixed integer nonlinear program (MINLP), wherein the travel cost for bridge links is a non-convex nonlinear function of retrofit decisions. In general, it is known that non-convex MINLPs can be notoriously difficult to solve [cf. 42]. Thus another contribution of this study stems from the algorithmic development. In particular, we propose a decomposition that is based on the generalized Benders decomposition (GBD) method [43]. As part of this decomposition, we present a convex reformulation of the recourse function in order to resolve the issues of non-separability of first and second stage variables. This enables us to efficiently generate Benders cuts for our decomposition algorithm. We justify our model and decomposition method on a hypothetical nine-node network and then apply the model and solution method to solve a stochastic transportation network protection problem based on the benchmark Sioux Falls network (cf. Figure 1). We use hazard events as a demonstration to explore the effects of risk

5

measures and variations in critical parameters on the optimal solutions.

The remainder of the paper is organized as follows. The mean-risk two-stage SP model is presented in section 2, followed by the convex reformulation of the recourse function in section 3. Our decomposition algorithm is described in section 4. Computational experiments on the two networks are carried out in section 5. The paper concludes along with a discussion of future research in section 6.

2. Mean-risk model

2.1. Parameters and variables

Let $G = (N, A)$ denote a transportation network, where N is the set of nodes and A is the set of directed arcs (or links) in the network. Denote by R and S, for some $R \neq \emptyset, S \subset N$, the set of origins and destinations in the network, respectively. The set of origin-destination (O-D) pairs is some subset $\mathcal{OD} \subseteq R \times S$. For every $(r, s) \in \mathcal{OD}$, $d^{rs} \in \mathbb{R}_+$ is the given travel demand on traffic originating at r and ending at s. Denote by $\bar{A}$, for some $\bar{A} \neq \emptyset, \bar{A} \subset A$, the set of links that are subject to hazards, which mainly comprises of the at-risk bridges. The nominal traffic capacity of each link $a \in A$ is equal to c_a. For $a \in A \setminus \bar{A}$, it is assumed that this link capacity remains unchanged after any disastrous event (e.g., natural or man-made disasters). However, the link capacities of links in $\bar{A}$ reduce due to the damage from the events and the extent of this change depends on how well the at-risk bridges were retrofitted before the events happened. The finite set H represents a list of applicable retrofit strategies for at-risk bridges in $\bar{A}$ in order to mitigate the adverse impacts caused by disastrous events in the future. The set H includes the do-nothing option and each at-risk bridge can be retrofitted with exactly only one strategy. The cost of retrofitting $a \in \bar{A}$ with strategy $h \in H$ is b_a^h. The total budget for retrofitting bridges is b_0.

In this study, we consider various hazard realizations, where each realization is a prediction of damage to the structure. Let the finite set K denote the set of hazard scenarios that the network is exposed to. Each scenario $k \in K$ is known to occur with a given probability $p_k \in (0, 1)$. For every $a \in \bar{A}, h \in H$, and scenario $k \in K$, we use the parameter $\theta_a^{h,k} \in (0, 1)$ to describe the ratio of post-event link capacity to the full link capacity, which can be determined externally by using bridge structural assessment, such as the study [44] for seismic damages. When disaster happens, the post-event capacity of link $a \in \bar{A}$ that was retrofitted with strategy $h \in H$ is equal to $c_a \theta_a^{h,k}$.

We now describe the decision variables used to construct our mathematical formulation. For every $a \in \bar{A}, h \in H$, the binary variable u_a^h is equal to 1 if and only if link a is retrofitted by strategy $h \in H$. For $(r, s) \in \mathcal{OD}, a \in A$ and $k \in K$, $x_a^{rs,k}$ is the flow on link a corresponding to the traffic originating at r and terminating at s for scenario k. The total flow on link $a \in A$ due to all O-D pairs is v_a^k, and $v_a^k = \sum_{(r,s) \in \mathcal{OD}} x_a^{rs,k}, \forall a \in A$. In this model, we allow unsatisfied post-disaster travel demand for various reasons, such as shutdown of certain roadways, acute increased traffic congestion in the network, etc. The unsatisfied travel demand for any O-D

6

pair (r, s) is captured by the decision variable $q^{rs,k}$ and we use a big-M to impose a penalty cost for the unsatisfied demand in the objective function.

Remark 1. In the transportation network literature, traffic is often assumed to be in a user-equilibrium condition, where no traveler can further reduce their travel cost by simply changing their own routing decision [45]. This assumption holds for a normal situation, where travelers have learned and adapted to daily traffic condition. However, modeling travelers' routing behavior in an environment following extreme events, such as earthquake, is still arguable [4]. In this paper, it is assumed that traffic flow can be controlled to achieve system-optimization and the resulting estimated travel cost can be considered as a lower bound of actual travel cost.

2.2. Two-stage stochastic models

2.2.1. Risk-neutral model

We first present a basic two-stage stochastic programming model for our problem. The first stage considers the retrofit resource allocation problem and decides the retrofitting strategy for each of the links in $\bar{A}$. Define the set U as

$$U := \left\{ u \in \{0,1\}^{|\bar{A}| \times |H|} \mid \sum_{h \in H} u_a^h = 1 \ \ \forall a \in \bar{A}, \ b^\top u \leq b_0 \right\} \tag{1}$$

to include all first-stage decisions — each link in $\bar{A}$ can be retrofitted with exactly one strategy and the total budget is b_0. The problem is to minimize[2] $b^\top u + \mathbb{E} \, Q(u, \omega)$. Here, $b^\top u$ is the total retrofitting cost and the recourse function $Q(u, \omega)$ is the incurred travel cost. Equivalently, the first-stage objective is to minimize $\mathbb{E} \, f(u, \omega)$, where

$$f(u, \omega) := b^\top u + Q(u, \omega) \tag{2}$$

is the total cost function. The assumption of finitely many scenarios indexed by the set K allows us to discretize the expected travel cost function and state our two-stage stochastic program as

$$(\text{2-stage SP}) : \quad \min_u \sum_{k \in K} p_k f^k(u) = \min_u \ b^\top u + \sum_{k \in K} p_k Q^k(u) \quad \text{s.t.} \quad u \in U, \tag{3}$$

where $f^k(u) = b^\top u + Q^k(u)$ is the total cost function for the kth scenario, in which $Q^k(u)$ is the optimal value for the total travel cost, given the retrofitting vector u. The recourse function is

---

[2]As is customary in literature, we use ω to denote scenarios for the non-discretized model.

based on an explicit traffic assignment model and for the kth scenario it is defined as

$$Q^k(u) = \min_{x^k, q^k} \quad \gamma \sum_{a \in A} v_a^k t_a^k \; + \; M \sum_{(r,s) \in \mathcal{OD}} q^{rs,k} \tag{4a}$$

$$= \min_{v^k, q^k, x^k} \quad \gamma \sum_{a \in A} t_{0a} \left[v_a^k + \delta \frac{(v_a^k)^5}{\hat{c}_a^k(u)^4} \right] \; + \; M \sum_{(r,s) \in \mathcal{OD}} q^{rs,k} \tag{4b}$$

$$\text{s.t.} \quad v_a^k = \sum_{(r,s) \in \mathcal{OD}} x_a^{rs,k} \quad \forall a \in A, \quad (x^k, q^k) \in X. \tag{4c}$$

In the second stage, v_a^k is the aggregation of link flow $x_a^{rs,k}$ over all O-D pairs (r,s), $q^{rs,k}$ is the unsatisfied demand between an O-D pairs (r,s), and

$$t_a^k = t_{0a} \left[1 + \delta \left(\frac{v_a^k}{\hat{c}_a^k(u)} \right)^4 \right] \quad \forall a \in A \tag{5}$$

is the link travel time per unit flow. The objective function (4a) is to minimize the total cost of traffic flow on the network and consists of two terms. Each product $v_a^k t_a^k$ is equal to the travel time for the entire flow on link $a \in A$ and upon scaling this with the parameter γ that converts travel time to a monetary value[3]. The second term represents the "penalty cost" for unsatisfied demand. In our second stage problem, unsatisfied travel demand is penalized for economic concerns and a big positive number M is used to represent peoples' willingness to travel. Compared to the value of time, peoples' willingness to travel is hard to calibrate and is beyond the scope of this study; we simply use a big number to penalize the unsatisfied demand. The link travel time per unit flow is usually a non-decreasing link performance function of the aggregated link flow and a non-increasing function of the post-event link capacity in each scenario. Equation (5) expresses the dependence of t_a^k on v_a^k using the Bureau of Public Records (BPR) function [46], in which t_{0a} is a parameter for the free-flow-speed travel time of link a, δ is an empirical data (e.g., 0.15), and the denominator $\hat{c}_a^k(u)$, which is a function of the first stage decision u, denotes the remaining link capacity on link a in scenario k:

$$\hat{c}_a^k(u) = \begin{cases} c_a \sum_{h \in H} \theta_a^{h,k} u_a^h & a \in \bar{A} \\ c_a & a \in A \setminus \bar{A}. \end{cases} \tag{6}$$

---

[3]In practice, determining the value of γ requires approximation of value of travel time savings, which is assumed to be equal to a nationwide median gross compensation for business travel (U.S. Department of Transportation, 2014).

The recourse function $Q^k(u)$ seeks to optimize flows over the set X, defined as:

$$X := \Big\{ (x,q) \geq (\mathbf{0},\mathbf{0}) \mid \sum_{j:\,(r,j)\in A} x_{rj}^{rs} - \sum_{j:\,(j,r)\in A} x_{jr}^{rs} + q^{rs} = d^{rs} \quad \forall (r,s) \in \mathcal{OD} \tag{7a}$$

$$\sum_{j:\,(s,j)\in A} x_{sj}^{rs} - \sum_{j:\,(j,s)\in A} x_{js}^{rs} - q^{rs} = -d^{rs} \quad \forall (r,s) \in \mathcal{OD} \tag{7b}$$

$$\sum_{j:\,(i,j)\in A} x_{ij}^{rs} - \sum_{j:\,(j,i)\in A} x_{ji}^{rs} = 0 \quad \forall (r,s) \in \mathcal{OD}, i \in N \setminus \{r,s\} \Big\}. \tag{7c}$$

For each O-D pair (r,s), equations (7a) and (7b) allow a slack of q^{rs} in the flow balance at r and s, respectively, to account for unsatisfied travel demand, whereas equation (7c) balances flow exactly at all other nodes in the network.

As the post-earthquake link capacity (6) is a linear function of retrofit decisions for links in $\bar{A}$, the decision variable u appears on the denominator of the travel time cost function in (5). This imparts non-convexity and nonlinearity to our two-stage stochastic problem and also leads to the following property.

Observation 1. *Problem (2-stage SP) has* complete recourse, *i.e., subproblem (4) is feasible for every $u \in U$.*

2.2.2. Mean-risk model

We now turn to introducing our mean-risk stochastic program, which combines the two-stage risk-neutral SP model and the CVaR function for risk assessment. Recall that the α-level CVaR of a random variable $\mathcal{Z}(\chi,\omega)$ is [cf. 34]:

$$\mathbb{CVaR}_\alpha \, \mathcal{Z}(\chi,\omega) := \inf_{\eta'} \; \left[\eta' + \frac{1}{1-\alpha} \mathbb{E} \max\left\{0, \mathcal{Z}(\chi,\omega) - \eta'\right\} \right]$$

$$= \eta + \frac{1}{1-\alpha} \mathbb{E} \max\left\{0, \mathcal{Z}(\chi,\omega) - \eta\right\},$$

where η denotes VaR. If $\mathcal{Z}(\chi,\omega)$ is the first stage cost of a stochastic program, the mean-risk objective is $\mathbb{E}\,\mathcal{Z}(\chi,\omega) + \lambda\,\mathbb{CVaR}_\alpha\,\mathcal{Z}(\chi,\omega)$, where the coefficient $\lambda \in [0,\infty)$ represents a trade-off between the risk measure (CVaR) and the expected first stage cost. Since $f(u,\omega) = b^\top u + Q(u,\omega)$ is the total cost function for our problem, the mean-risk objective for us is $\mathbb{E}\,f(u,\omega) + \lambda\,\mathbb{CVaR}_\alpha\,f(u,\omega)$. The risk-neutral problem (2-stage SP) corresponds to $\lambda = 0$. Upon discretizing with finitely many scenarios as before, performing simple manipulations arising out of translation invariance of CVaR, and linearizing the $\max\{0,\cdot\}$ function in CVaR,

9

the mean-risk stochastic program becomes

$$
\begin{aligned}
(\text{Mean-risk SP}) : \quad \min_{u,\eta,\xi} \quad & (1+\lambda)b^\top u \; + \; \sum_{k \in K} p_k Q^k(u) \; + \; \lambda \left(\eta + \frac{1}{1-\alpha} \sum_{k \in K} p_k \xi^k \right) && \text{(8a)} \\
\text{s.t.} \quad & u \in U && \text{(8b)} \\
& \xi^k \ge Q^k(u) - \eta \;\; \forall k \in K && \text{(8c)} \\
& \xi^k \ge 0 \;\; \forall k \in K, && \text{(8d)}
\end{aligned}
$$

where $Q^k(u)$ is defined by equations (4)–(6). The objective is to minimize the total cost of retrofitting bridges, expected travel cost, unsatisfied demand penalty and the risk term. Here λ is a pre-defined weighting factor. A larger λ value leans towards CVaR and thus results in a more conservative solution. On the other hand, a smaller λ value yields a solution that weighs more on the expected cost, and thus the solution is more risk-neutral.

3. Recourse function

For each scenario k, the recourse function $Q^k(u)$ is a nonlinear optimization problem in (4). This problem is *non-convex* due to presence of the bilinear terms $v_a^k t_a^k$ in the objective and nonlinear equality constraints defining t_a^k. More importantly, since the fractional function $\frac{v_a}{\tilde{c}_a^k(u)}$ in (5) has u appearing linearly in the denominator, the second stage variables are *non-separable* from the first stage variable in this formulation. Problem convexity and separability of the variables are both desirable properties of Benders-type decomposition methods for solving a two-stage stochastic program with a nonlinear second stage since they guarantee generation of valid supporting hyperplanes of the recourse function [cf. 43, 47]. Our decomposition algorithm for solving (Mean-risk SP) is presented in §4. In this section, we derive a reformulation of $Q^k(u)$ in (4b) that is not only a convex program for every $u \in U$ but also achieves separability between first and second stage variables. This reformulation leads to a convex MINLP formulation for solving (Mean-risk SP) as a single optimization problem.

For a fixed $u \in U$, the recourse value $Q^k(u)$ can be obtained by solving the convex optimization problem (4). However this does not tell us anything about the convexity of $Q^k(\cdot)$. We exploit properties of the discrete set U to show that the recourse function is indeed convex. Our main approach is to eliminate u from the denominator in (4b) and make the subproblem separable in first and second stage variables. In particular, we obtain subproblem constraints that are linear in u, convex in v and do not contain product terms between u and any of v, q, x. There are different ways of achieving this and we present these next.

Let us introduce a auxiliary second stage non-negative continuous variable y_a^k for each $a \in \bar{A}$ and add the inequality

$$
y_a^k \ge \frac{(v_a^k)^5}{(c_a \sum_{h \in H} u_a^h \theta_a^{h,k})^4} \quad \forall a \in \bar{A}. \tag{9}
$$

10

The right hand side of the above inequality appears in the objective (4b) with a positive coefficient $\gamma \delta t_{0a}$. Hence we have

$$Q^k(u) = \min_{v^k, q^k, x^k, y^k} \quad \gamma \sum_{a \in A} t_{0a} \left[v_a^k + \delta y_a^k \right] + M \sum_{(r,s) \in \mathcal{OD}} q^{rs,k} \tag{10a}$$

$$\text{s.t.} \quad (4c), (9). \tag{10b}$$

The following lemma guides our convex reformulation for $Q^k(u)$.

Lemma 1. *For $a \in \bar{A}$ and $u \in U$, $\left(\sum_{h \in H} \theta_a^{hk} u_a^h \right)^\beta = \sum_{h \in H} \left(\theta_a^{hk} \right)^\beta u_a^h$ for all $\beta \in \mathbb{R}$.*

The proof is straightforward. Since $\sum_{h \in H} u_a^h = 1$ and $u_a^h \in \{0, 1\}$, it must be that for every $a \in \bar{A}$, we have $u_a^h = 1$ for some $h \in H$ and $u_a^{h'} = 0$ for all $h' \in H \setminus \{h\}$. Hence both $(\sum_{h \in H} \theta_a^{hk} u_a^h)^\beta$ and $\sum_{h \in H} (\theta_a^{hk})^\beta u_a^h$ are equal to $(\theta_a^{hk})^\beta$.

After clearing the denominator in (9) and applying Lemma 1 with $\beta = 4$, we obtain

$$(v_a^k)^5 \le c_a^4 \left[\sum_{h \in H} \left(\theta_a^{hk} \right)^4 u_a^h \right] y_a^k \quad \forall a \in \bar{A}. \tag{11}$$

Remark 2. For $u \in U$, since $\sum_h u_a^h = 1$ and $u_a^h \in \{0, 1\}$, the term $\sum_{h \in H} \left(\theta_a^{hk} \right)^4 u_a^h$ can be interpreted as the unary expansion of a discrete variable that takes values in the finite set $\cup_h \{ \left(\theta_a^{hk} \right)^4 \}$. The right hand side of inequality (11) is then the product of a discrete variable and a non-negative continuous variable and is therefore a bilinear term. Another formulation for this bilinear term can be obtained using the binary expansion of the discrete variable, where only $\log_2 |H|$ many $\{0, 1\}$ variables (as opposed to $|H|$ $\{0, 1\}$ u's in the unary case) are required. Gupte et al. [48] theoretically compared unary and binary expansion reformulations for bilinear optimization problems, obtained new valid inequalities to strengthen the continuous relaxation of the binary reformulation and showed that these convexifications work well on hard test instances. This encourages the use of binary expansion formulations for general bilinear problems. However, in our case since the cardinality of H is quite small (e.g., 5), the discrete variable takes only up to 5 different values and there is no significant benefit of adopting the logarithmic formulation for $\cup_h \left(\theta_a^{hk} \right)^4$. Therefore we choose to not modify the term $\sum_{h \in H} \left(\theta_a^{hk} \right)^4 u_a^h$ in (11).

In mixed integer nonlinear optimization literature, it is common practice to replace each nonlinear constraint of $\le$-type with the convex envelope of the corresponding nonlinear function; see Tawarmalani and Sahinidis [49]. Such a replacement usually relaxes the nonlinear constraint, although if some of the variables are discrete, one may sometimes also obtain an exact reformulation of the constraint. The $\le$-inequality in (11) has different sets of variables on the left and right hand sides. Therefore, if we write the constraint as the difference of the left and right hand sides, taking the convex envelope of this difference is equivalent to separately taking the convex envelope of the left hand side and the concave envelope of the right hand

11

side. The left hand side in (11) is a univariate convex function of v_a over $\mathbb{R}_+$ and hence does not require any convexification. For the right hand side, we have a bilinear term between a discrete variable $\sum_{h \in H} \left(\theta_a^{hk}\right)^4 u_a^h \in \cup_h \left\{ \left(\theta_a^{hk}\right)^4 \right\}$ (cf. Remark 2) and a continuous variable y_a^k. The concave envelope of this bilinear term is given by its McCormick inequalities [50], which depend on lower and upper bounds on the variables appearing in the bilinear term. The bounds for $\sum_{h \in H} \left(\theta_a^{hk}\right)^4 u_a^h$ and y_a^k can be obtained as follows. It is clear that for $u \in U$,

$$\underline{\theta}_a^k \leq \sum_{h \in H} \left(\theta_a^{hk}\right)^4 u_a^h \leq \bar{\theta}_a^k, \quad \text{where} \quad \underline{\theta}_a^k := \left(\min_{h \in H} \theta_a^{hk}\right)^4, \ \bar{\theta}_a^k := \left(\max_{h \in H} \theta_a^{hk}\right)^4.$$

From equations (4c) and (9) we get the lower bound on y_a^k to be zero. For every $a \in \bar{A}$, let $\varsigma_a > 0$ be a large enough positive constant such that every optimal solution to (10) satisfies $v_a \leq c_a \varsigma_a \ \forall a \in \bar{A}$. Then by inequality (9) and Lemma 1, every optimal solution to (10) satisfies

$$y_a^k \leq \frac{c_a \varsigma_a^5}{\sum_h (\theta_a^{hk})^4 u_a^h} \tag{12a}$$

which leads to

$$y_a^k \leq \frac{c_a \varsigma_a^5}{\underline{\theta}_a^k} \tag{12b}$$

since $u \in U$. Using these lower and upper bounds, the McCormick concave envelope of the bilinear term on the right hand side of (11) is

$$c_a^4 \min \left\{ \bar{\theta}_a^k y_a^k, \ \underline{\theta}_a^k y_a^k + \frac{c_a \varsigma_a^5}{\underline{\theta}_a^k} \sum_{h \in H} \left(\theta_a^{hk}\right)^4 u_a^h - c_a \varsigma_a^5 \right\}. \tag{13}$$

and hence we have two inequalities for (11):

$$(v_a^k)^5 \leq c_a^4 \bar{\theta}_a^k y_a^k, \quad (v_a^k)^5 \leq c_a^4 \underline{\theta}_a^k y_a^k + \frac{(c_a \varsigma_a)^5}{\underline{\theta}_a^k} \sum_{h \in H} \left(\theta_a^{hk}\right)^4 u_a^h - (c_a \varsigma_a)^5 \qquad \forall a \in \bar{A}. \tag{14}$$

Gupte et al. [48, Proposition 2.1] tells us that modeling a bilinear term between a general integer and a continuous variable with the McCormick inequalities allows for more integer solutions. The same holds true when the bilinear term is between a general discrete and a continuous variable. Therefore (14) yields a relaxation but not a reformulation of (11). Although this relaxation can be used to under-estimate the recourse function $Q^k(u)$, doing so will only yield weaker cuts in the decomposition algorithm.

In order to derive an exact reformulation of (11), first note that $(v_a^k, (u_a^h)_h, y_a^k)$ is feasible

12

to (11) if and only if there exists some w_a^k such that

$$(v_a^k)^5 \leq c_a^4 w_a^k, \tag{15a}$$

$$0 \leq w_a^k \leq c_a \varsigma_a^5, \quad w_a^k \leq \left[\sum_{h \in H} \left(\theta_a^{hk} \right)^4 u_a^h \right] y_a^k. \tag{15b}$$

This equivalence is correct because $0 \leq v_a \leq c_a \varsigma_a$ implies that the left hand side of (11) is upper-bounded by $(c_a \varsigma_a)^5$. Since $c_a \varsigma_a^5 < c_a \varsigma_a^5 \bar{\theta}_a^k / \underline{\theta}_a^k$ and the right hand side is the product of the upper bounds on $\sum_{h \in H} \left(\theta_a^{hk} \right)^4 u_a^h$ and y_a^k, respectively, it is clear that the upper bound on w_a^k is nontrivial. We will convexify $(15b)$ to obtain a strong reformulation of (11).

Remark 3. Inequalities (14) are precisely the projection of the McCormick relaxation of

$$v_a^5 \leq c_a^4 w_a^k, \quad 0 \leq w_a^k \leq \left[\sum_{h \in H} \left(\theta_a^{hk} \right)^4 u_a^h \right] y_a^k, \tag{16}$$

where the bilinear term is relaxed using (13). Observe that (15) and (16) are each equivalent to (11) but (16) is a relaxation of (15) in the $(v_a^k, (u_a^h)_h, y_a^k, w_a^k)$-space. Therefore convexifying $(15b)$ produces a stronger reformulation in the $(v_a^k, (u_a^h)_h, y_a^k, w_a^k)$-space than convexifying $0 \leq w_a^k \leq \left[\sum_{h \in H} \left(\theta_a^{hk} \right)^4 u_a^h \right] y_a^k$ in (16) and hence could lead to stronger cuts in the decomposition algorithm.

Equation $(15b)$ represents a bounded product term between a discrete and a continuous variable and for such bilinear terms, we note that the McCormick envelopes are neither a reformulation nor do they yield the convex hull.

Observation 2. *Denote* $\mathcal{I} := \{b_1, b_2, \ldots, b_m\} \times [0, d] \times [0, \eta]$ *with* $m \geq 3, 0 \leq b_1 < b_2 < \cdots < b_m$ *and* $\eta < b_m d$. *Let* $\mathcal{R} := \{(x, y, \nu) \in \mathcal{I} \mid \nu \leq xy\}$, $\mathcal{M} := \{(x, y, \nu) \in \mathcal{I} \mid \nu \leq b_m y, \ \nu \leq b_1 y + dx - db_1\}$ *be the McCormick relaxation of* $\mathcal{R}$, *and* $\mathcal{M}' := \{(x, y, \nu) \in [b_1, b_m] \times [0, d] \times [0, \eta] \mid \nu \leq b_m y, \ \nu \leq b_1 y + dx - db_1\}$ *be the continuous relaxation of* $\mathcal{M}$. *Then* $\mathcal{R} \subsetneq \mathcal{M}$ *and* $\mathrm{conv} \, \mathcal{R} \subsetneq \mathcal{M}'$.

Proof. $\mathcal{M}$ being the McCormick relaxation of $\mathcal{R}$ leads to $\mathcal{R} \subseteq \mathcal{M}$ and $\mathrm{conv} \, \mathcal{R} \subseteq \mathcal{M}'$. Denote

$$\chi_0 := \frac{d}{\eta(1 - \frac{b_1}{b_m})}, \quad \chi_1 := \eta \min\{1, (b_2 - b_1)\chi_0\}.$$

Then $(b_2, \frac{\chi_1}{b_m}, \chi_1) \in \mathcal{M} \setminus \mathcal{R}$. Note that $(b_1 + \frac{1}{\chi_0}, \frac{\eta}{b_m}, \eta)$ is an extreme point of $\mathcal{M}'$. Suppose this point can be written as a nontrivial convex combination of finitely many $(x^t, y^t, \nu^t) \in \mathcal{R}$. Then $\nu^t = \eta \ \forall t$. Since $\nu^t \leq x^t y^t$ and $x^t \leq b_m$, it follows that $y^t \geq \eta / b_m$ and hence $y^t = \eta / b_m$ and $x^t = b_m$ for all t. Consequently, $b_1 + \frac{1}{\chi_0} = b_m$, which is a contradiction because $\eta < b_m d$ by assumption. $\qquad \square$

An extended formulation for the convex hull of $\mathcal{R}$ can be obtained using unary expansion of

discrete variables. Let $\nu = \sum_i b_i z_i$ with $\sum_i z_i = 1$, $z_i \in \{0, 1\}$ $\forall i$. Then disjunctive programming [51] implies that conv $\mathcal{R}$ is equal to the projection onto the (x, y, ν)-space of the polyhedron

$$\Big\{ (x, y, \nu, z) \mid x = \sum_{i=1}^{m} b_i z_i, \ \nu = \sum_{i=1}^{m} \nu^i, \ y = \sum_{i=1}^{m} y^i$$
$$0 \leq y^i \leq dz_i, \ 0 \leq \nu^i \leq \delta z_i, \ \nu^i \leq b_i y^i \quad \forall i \tag{17}$$
$$\sum_{i=1}^{m} z_i = 1, \ z_i \geq 0 \ \forall i \Big\}.$$

Since $\sum_h (\theta_a^{hk})^4 u_a$ is the unary expansion of a discrete variable as mentioned in Remark 2, we may apply (17) directly to (15b). However, we will first strengthen the bounds on the y_a^k variables in each disjunction. Of the two upper bounds on y_a^k in (12a) and (12b), the former is stronger but is a function of u whereas the latter is weaker but is a constant. The constant bound in (12b) is necessary for deriving McCormick relaxations of bilinear terms as in Observation 2. The bound in (12a) can be incorporated into the disjunctive programming approach of equation (17). Since $y_a^k \leq \frac{c_a \varsigma_a^5}{\sum_h (\theta_a^{hk})^4 u_a^h}$ by equation (12a) and $\sum_h u_a^h = 1$ and $u_a^h \in \{0, 1\}$ $\forall h$ for every $u \in U$, it is clear that convexifying (15b) is equivalent to convexifying the following finite union of polytopes:

$$\bigcup_{h \in H} \Big\{ (u_a, y_a^k, w_a^k) \mid u_a = \mathbf{e}_h, \ 0 \leq y_a^k \leq \frac{c_a \varsigma_a^5}{(\theta_a^{hk})^4}, \ 0 \leq w_a^k \leq c_a \varsigma_a^5, \ w_a^k \leq c_a^4 (\theta_a^{hk})^4 y_a^k \Big\}. \tag{18}$$

where $\mathbf{e}_h$ is the hth coordinate unit vector. A straightforward application of disjunctive programming [51] gives us the convex hull of (18), and hence that of (15b), thereby resulting in a strong reformulation of the recourse function, which we state next.

Proposition 1. *The recourse function of the kth scenario can be formulated as:*

$$Q^k(u) = \min_{\substack{v^k, q^k, x^k \\ y^k, w^k}} \ \gamma \sum_{a \in A} t_{0a} \Big[v_a^k + \delta y_a^k \Big] \ + \ M \sum_{(r,s) \in \mathcal{OD}} q^{rs,k} \tag{19a}$$

$$\text{s.t.} \quad v_a^k = \sum_{(r,s) \in \mathcal{OD}} x_a^{rs,k} \ \ \forall a \in A, \quad (x^k, q^k) \in X \tag{19b}$$

$$(v_a^k)^5 \leq c_a^4 \sum_{h \in H} w_a^{hk}, \ y_a^k = \sum_{h \in H} y_a^{hk} \quad \forall a \in \bar{A} \tag{19c}$$

$$w_a^{hk} \leq c_a^4 (\theta_a^{hk})^4 y_a^{hk} \quad \forall h \in H, a \in \bar{A} \tag{19d}$$

$$0 \leq y_a^{hk} \leq \frac{c_a \varsigma_a^5}{(\theta_a^{hk})^4} u_a^h, \ 0 \leq w_a^{hk} \leq c_a \varsigma_a^5 u_a^h \quad \forall h \in H, a \in \bar{A} \tag{19e}$$

where for every $a \in \bar{A}$, ς_a is a large enough positive constant such that $c_a \varsigma_a$ is the upper-bound

14

on the traffic volume of link a.

Notice that Proposition 1 linearly separates the first stage variable u from the second stage variables. This implies that the recourse function $Q^k(u)$ is convex in u and can be approximated by supporting hyperplanes. It also implies a convex MINLP formulation for the mean risk problem (8).

$$
\begin{aligned}
(\textsf{Convex MINLP}): \quad & \min_{\substack{u,\eta,\xi \\ v,q,x,y,w}} \quad (1+\lambda)b^\top u \;+\; \sum_{k\in K} p_k \left[\gamma \sum_{a\in A} t_{0a}\left[v_a^k + \delta y_a^k \right] \;+\; M \sum_{(r,s)\in\mathcal{OD}} q^{rs,k} \right] \\
& \qquad\qquad + \lambda \left(\eta + \frac{1}{1-\alpha} \sum_{k\in K} p_k \xi^k \right) \\
& \text{s.t.} \quad u \in U, \quad \xi^k \geq 0 \;\; \forall k \in K \\
& \qquad\quad \xi^k \geq \gamma \sum_{a\in A} t_{0a}\left[v_a^k + \delta y_a^k \right] \;+\; M \sum_{(r,s)\in\mathcal{OD}} q^{rs,k} \;-\; \eta \;\; \forall k \in K \\
& \qquad\quad (19\mathrm{b}) - (19\mathrm{e}) \;\; \forall k \in K
\end{aligned}
$$

This convex MINLP can be solved to ϵ-optimality using state-of-the-art MINLP solvers. However we demonstrate in §5 that even on a simple nine-node network, these generic global optimization solvers take a long time to converge, thereby making this approach intractable for larger-sized practical instances. This motivates our algorithmic approach in the next section.

4. Decomposition method

Extensive algorithmic efforts have been made to improve the efficiency of solution algorithms for MINLPs, including the widely used branch and bound [52] with its variants — LP/NLP based branch and bound method [53] and spatial branch and bound [54], as well as Generalized Benders Decomposition (GBD) method [43]. The branch and bound method is an implicit enumeration procedure and can be computationally expensive when the number of integer variables is large. The GBD, on the other hand, can be effective in handling computationally challenging MINLPs by decomposing them to smaller tractable subproblems. In this study, we apply a decomposition method based on GBD. Also note that there are other plausible solution methods, including Extended Cutting Plane method [55], and outer approximation [56]. Though beyond the scope of this study, comparisons between these different methods in terms of solution quality and performance are worthy of investigation in future works.

The mean-risk SP model (8) is decomposed into a master problem and one subproblem for each scenario k. The master problem is a mixed $0\backslash 1$ linear program (MILP) and contains first-stage integer variables u and the value-at-risk η. The sub-problems are evaluated for the second-stage cost, given the first-stage variable u. Combined with the first-stage cost, we can compute CVaR for the overall cost at the optimum of the master problem. We will discuss the details of our decomposition method in this section.

15

GBD was proposed by Geoffrion [43] and a detailed exposition on it can be found, for example, in Floudas [47]. In this method, when the first stage variables are temporally held fixed, the remaining optimization problem is considerably more tractable than the original one. As for this study, if bridge retrofit decision variable u and the value-at-risk η are temporarily fixed, the remaining problem (4) becomes a traffic assignment problem based on system-optimization condition, which may be effectively solved by using commercial nonlinear program solvers. The CVaR value can be obtained once we have travel cost function values from the traffic assignment problems corresponding to different scenarios.

In the objective function of the master problem, the recourse function travel cost and CVaR are not known explicitly in advance. Thus, two optimality cuts are added iteratively to approximate them. At iteration i, let $\pi^{ki}u \geq \pi_0^{ki}$ be a cut that lower approximates $Q^k(u)$. Then the master problem at any iteration l reads as

$$\text{(Master)}: \quad \min_{u,\eta,\xi,\phi_1} \quad (1+\lambda)b^\top u + \phi_1 + \lambda \left(\eta + \frac{1}{1-\alpha} \sum_{k \in K} p^k \xi^k \right)$$

$$\text{s.t.} \quad u \in U, \quad \xi^k \geq 0 \ \ \forall k \in K$$

$$\text{Optimality cut 1} \quad \phi_1 \geq \sum_k p_k(\pi^{ki}u - \pi_0^{ki}) \quad i = 1, 2, \ldots, l$$

$$\text{Optimality cut 2} \quad \xi^k \geq \pi^{ki}u - \pi_0^{ki} - \eta \quad \forall k \in K,\, i = 1, 2, \ldots, l$$

The exact forms of these optimality cuts are presented in Proposition 2. According to Observation 1, the general problem has *complete recourse* and the feasibility cut constraint can thus be omitted.

Let $(\bar{u}, \bar{\eta}, \bar{\xi}, \bar{\phi}_1)$ be an optimal solution to the master problem. If $\bar{\phi}_1 < \sum_{k \in K} p_k Q^k(\bar{u})$, then optimality cut 1 will be added to the master problem. If $\sum_{k \in K} p_k \bar{\xi}^k < \sum_{k \in K} p_k \max\{0, Q^k(\bar{u}) - \bar{\eta}\}$, then optimality cut 2 will be added to the master problem. These optimality cuts are generated using Lagrange multipliers for each subproblem, which is a convex nonlinear problem, with u fixed to $\bar{u}$.

$$\text{(Subproblem } k): Q^k(\bar{u}) = \min_{\substack{v^k, q^k, x^k \\ y^k, w^k}} \quad (19a)$$

$$\text{s.t.} \quad \text{constraints (19b)} - (19d)$$

$$0 \leq y_a^{hk} \leq \frac{c_a \varsigma_a^5}{(\theta_a^{hk})^4} \bar{u}_a^h, \ 0 \leq w_a^{hk} \leq c_a \varsigma_a^5 \bar{u}_a^h \quad \forall h \in H, a \in \bar{A}$$

The convex reformulation of $Q^k(u)$ in Proposition 1 and the arguments thereafter imply that it is straightforward to apply the GBD method for generating optimality cuts in the master problem.

Proposition 2. *Let $\bar{u}^l$ be an optimum solution of the master problem at l^{th} iteration. For each scenario k, let μ^{kl} and λ^{kl} be vectors of optimum Lagrange multipliers for the last two sets of constraints in subproblem $Q^k(\bar{u}^l)$. Denote*

$$\bar{y}_a^{hk} := \frac{c_a \varsigma_a^5}{(\theta_a^{hk})^4} \quad h \in H, a \in \bar{A}.$$

Then the optimality cuts for the lth iteration are:

$$\phi_1 \geq \sum_{k \in K} p_k [Q^k(\bar{u}^l) - \mu^{kl}\bar{y}^k(u - \bar{u}^l) - \lambda^{kl}c_a\varsigma^5(u - \bar{u}^l)] \tag{20a}$$

$$\xi^k \geq Q^k(\bar{u}^l) - \mu^{kl}\bar{y}^k(u - \bar{u}^l) - \lambda^{kl}c_a\varsigma^5(u - \bar{u}^l) - \eta \quad \forall k \in K \tag{20b}$$

Proof. Proposition 1 linearly separates the first stage variable u from the second stage variables, i.e., the subproblem constraints in (19e) are the only ones containing both first and second stage variables and these can be represented as $h_1(u) + g_1(w) \leq 0$ or $h_2(u) + g_2(y) \leq 0$ where h_1, h_2, g_1, g_2 are all linear functions. This structure fits in with the so-called P-property of GBD [cf. 47, §6.3.5.1], allowing for a straightforward application of GBD and thereby leading to the proposed optimality cuts. $\qed$

Multiple optimality cuts may help improve algorithm efficiency. Readers may refer to Birge and Louveaux [15] for details. The multi-cut version of optimality cut for (20a) is

$$\phi_1^k \geq Q^k(\bar{u}^l) - \mu^{kl}\bar{y}^k(u - \bar{u}^l) - \lambda^{kl}c_a\varsigma^5(u - \bar{u}^l) \tag{21}$$

Accordingly, we should use the aggregation of cuts $\sum_{k \in K} p^k \phi_1^k$ to replace ϕ_1 in the objective function of (Master). Note that due to the CVaR function definition, optimality cut (20b) is already in multi-cut version. In each iteration, there are $|K|+1$ constraints added to the master problem, consisting of $|K|$ constraint (20b) and one constraint (20a).

The decomposition algorithm procedure:

1. Initialization $l = 0$.
2. Solve (Master). Let $(\bar{u}, \bar{\eta}, \bar{\xi}, \bar{\phi}_1, \bar{\phi}_2)$ be optimal solution and set $\bar{\phi} = \bar{\phi}_1 + \lambda(\bar{\eta} + \frac{1}{1-\alpha}\sum_k p_k\bar{\xi}^k)$.
3. Fix $u = \bar{u}$ and solve (Subproblem k) for all $k \in K$. Set $l = l + 1$ and calculate

$$\phi^* = \sum_{k \in K} p^k Q^k(\bar{u}) + \lambda \, \mathbb{CVaR}_\alpha \, Q(\bar{u}).$$

4. The procedure terminates if the optimality gap $|1 - \dfrac{\bar{\phi}}{\phi^*}| \leq \epsilon$ (ϵ is a predefined small value) is met. Optimal solution is found. Otherwise, add optimality cuts (20a) (or the multi-cut version (21)) and (20b) to the master problem, and go back to step 2.

5. Numerical examples

The proposed mean-risk model and decomposition methods are first validated using a hypothetical small nine-node network. The Sioux-Falls network is then used to explore the impacts of uncertainty, network topology, and critical parameters on the strategic decisions on highway bridge retrofits. All instances were programmed in AMPL. For our decomposition, the master problem was solved as a MILP with CPLEX and with the multi-cut version of optimality cuts, and each subproblem was solved as a convex nonlinear program with CONOPT.

5.1. Nine-node network

The nine-node network is shown in Figure 2. It consists of nine nodes, 24 directional links, and 72 (= 8×9) O-D pairs. Assume that three bridges on both directions on the network, labeled as A, B, and C, are vulnerable to seismic disasters and their post-disaster capacities may be reduced while other road links are assumed intact. The nine-node instances were tested on a desktop with 8 GB RAM and Intel Core i5-2500@3.40GHz processor under Windows 7 environment.
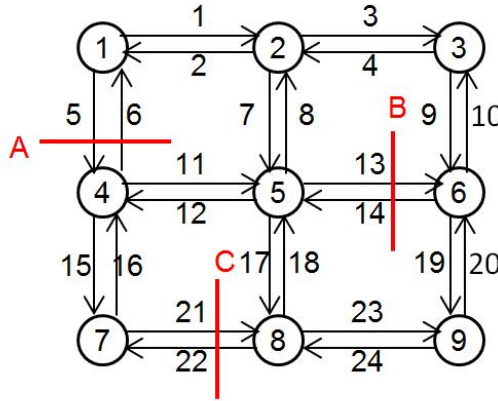

Figure 2: Nine-node network

The parameter $\theta_a^{h,k}$ is the ratio of bridge remaining capacity to the full capacity, which depends on the specific scenario, location of the bridge, and the retrofit strategies applied. Five strategies, denoted as $h_0 - h_4$, are considered. The "do nothing" strategy is h_0 and a higher index indicates a more robust, and hence more costly, strategy. In this experiment, we randomly generated $\theta_a^{h,k} \in (0,1]$ while ensuring that a higher numbered strategy results in a higher value of $\theta_a^{h,k}$. As a demonstration, Table 1 reports the ratios for one scenario. The initial values for all second-stage variables are set to be zero. The initial solution for the first-stage decision variable u is set as follows: for every $a \in \bar{A}$, $u_a^{h_0} = 1$ and $u_a^h = 0$ for $h \neq h_0$. Other critical parameters are: $\alpha = 0.7, \gamma = 1000, \lambda = 1$, and $\bar{y} = 1000$.

Two recent papers [57, 58] demonstrate that commercial MINLP solvers can successfully solve nonlinear, discrete transportation problems. We obtained benchmark solutions by using two commercial solvers — BONMIN [59] and FilMINT [60], to justify our decomposition method by using the small-scale network. We tested the model using four different sizes of scenario sets. In each set, scenarios are randomly generated to create variations in uncertainty realizations in order to justify the effects of CVaR.

Table 2 compares optimal objective values and solution times for the MINLP solvers and our decomposition algorithm (column GBD). As is to be expected, the objective values are almost identical for all three methods. The solution times using GBD are always substantially smaller than those using BONMIN and FilMINT. One may also notice that the increase in the number of scenarios does not necessarily translate to more GBD iterations. With more scenarios, more sub-problems need to be solved in each iteration, thereby GBD takes longer total time to finish. This explains why the solution time for GBD is almost identical when solving 12, 18, 24 scenarios even though the number of iterations was smallest in the case of 24 scenarios compared to the 12 and 18 scenarios. The experimental results in Table 2 justify the use of our proposed decomposition for large scaled problems, such as the Sioux Falls network.

Table 1: Sample values of $\theta_a^{h,k}$ for a fixed scenario k.

Link	Strategy				
	h_0	h_1	h_2	h_3	h_4
link5	0.05	0.5	0.5	0.5	1
link6	0.05	0.5	0.5	0.5	1
link13	0.5	0.5	0.5	0.75	0.75
link14	0.5	0.5	0.5	0.75	0.75
link21	0.17	0.33	0.33	0.67	0.67
link22	0.17	0.33	0.33	0.67	0.67

Table 2: Comparisons between GBD and MINLP solvers with $\alpha = 0.7, \lambda = 1$.

Scenarios	Obj. Value ($\times 10^6$)			CPU seconds			GBD iterations
	BONMIN	FilMINT	GBD	BONMIN	FilMINT	GBD	
6	466.416	466.416	466.416	1280	466	7	15
12	466.144	466.144	466.144	3754	2487	21	29
18	462.063	462.063	462.063	6340	4673	21	21
24	460.483	460.483	460.484	4315	11377	22	18

19

5.2. Sioux Falls network

The Sioux Falls network in Figure 1 consists of 24 nodes, 76 links, and 552 O-D pairs. The trip demands between all O-D demands are adopted from [6]. We adopted critical parameters from Fan et al. [7], including the peak 2-hour conversion value $\gamma = 2400$ to convert peak 2-hour delay to a monthly monetary value loss, which is set as $8 \times 30 \times 10 = 2400$, where 8 is the daily adjust factor with 30 days duration and 10 is the value of travel time savings for drivers. We used $\epsilon = 0.5\%$ for optimality gap tolerance to terminate the GBD algorithm. The instances were programmed in AMPL and run on a Linux cluster node with 16 Intel Cores and a total 64 GB RAM.

An engineering method to estimate earthquake damage of structures uses discrete damage states [61]; that is, the residual post-earthquake capacity ratio $\theta_a^{h,k}$ has discrete values. There are currently no publicly-available datasets for estimating the post-earthquate damage states for a given road network. Because collecting such data is beyond the scope of this study, we randomly generated $\theta_a^{h,k}$ such that there are substantial variations among different scenarios to justify the use of stochastic programming method in our study.

That being said, we develop a simple mechanism to generate $\theta_a^{h,k}$ in two steps. First, we consider three levels of damages, which are low, medium, and high damages and assume that the damages to the bridges at risk are independent. For a low-damage scenario k, we select five values for $\theta_a^{h,k}$ at random from $\{1/N, 2/N, \ldots, (N-1)/N, 1\}$ (we used $N = 6$ in this study). For medium and high damage scenarios, we pick five numbers randomly from $\{1/N, 2/N, \ldots, (N-1)/N\}$ and $\{1/N, 2/N, \ldots, (N-2)/N\}$, respectively. Note that $\theta_a^{h,k}$ under a low-damage scenario has larger range of numbers to choose from than $\theta_a^{h,k}$ under medium and high damage scenarios. Statistically, bridge residual capacity under high-damage scenarios is lower than that under low-damage scenarios for the same bridge. However, due to the complexity involved in the estimation, such as locations and structures of different bridges, there are inevitable fluctuations in the residual capacities, which are captured in our scenario generation mechanism. Also, for any bridge a under scenario k, the $\theta_a^{h,k}$ value should be non-decreasing with an enhanced (i.e., higher numbered strategy) strategy h, i.e., $\theta_a^{h_{i+1},k} \geq \theta_a^{h_i,k}$ for $i = 0, \ldots, 3$. Based on this, we assign the selected five numbers for $\theta_a^{h,k}$ according to the different retrofit strategies. We also assume that the occurrences of the three categories of scenarios follow a predefined ratio. For example, if a ratio of 5:3:2 is assumed for low-, median- and high-damage scenarios, respectively, for a total of 20 scenarios, the occurrences of each category of scenarios will be 10, 6, 4, respectively. The probabilities associated with scenarios are randomly generated from a uniform distribution.

We adopted the same five-strategy scheme (i.e., $h_0 - h_4$) and initial value settings from the nine-node network example. Since the Sioux falls network is much larger in size than the hypothetical nine-node network from section 5.1 and the experiments in Table 2 convinced us of the superiority of a decomposition approach over MINLP solvers, we obtained results using only our GBD method. Next, we explore the impacts of uncertainty, network topology, and critical parameters on the retrofit strategies from our numerical experiments.

20

5.2.1. Effects of risk parameters λ, α and scenarios K

The parameters α and λ reflect the decision makers' risk preferences. We tested $\alpha=$ 0.7, 0.8, 0.9 and 0.95 and λ = 0.1, 0.5, 1, and 100 with $\overline{y}$ = 1500 for 20, 50, and 100 scenarios. The time limit was set to 24 hours. The confidence level parameter α controls the set of scenarios to be considered while the coefficient λ weighs the CVaR in the integrated mean-risk stochastic model. Through the numerical experiments, we intend to (i) understand the effects of risk parameters on system costs; and (ii) highlight the modeling insights of a risk (i.e., CVaR) integrated stochastic program compared to a risk-neutral stochastic model.

Let us first investigate the breakdown of the total cost plotted in Figure 3 based on the result of 20 scenarios. For the purpose of this illustration, we experimented with ten different values for α. The total mean-risk cost or objective value is the sum of total expected costs and weighted CVaR. The total expected cost can be further decomposed into the retrofit cost and the expected travel cost. The impacts of the risk parameters on the cost effectiveness and CVaR will be discussed separately. Note that α represents the risk preference, which quantifies the mean value of the worst $(1 - \alpha)\%$ of the total costs. In Figure 3a, CVaR increases as α increases as per the definition, i.e., a larger value of α accounts for larger realizations of the total cost, while decreasing as λ increases. The total expected cost shown in Figure 3b is comprised of the retrofit cost in Figure 3c and the expected travel cost in Figure 3d. The results show that increasing both λ and α generally increases retrofit cost, because it results in a more risk-averse policy with enhanced and more costly retrofit strategies. As a result, we expect a reduced expected travel cost, which implies a lower post-disaster capacity loss. However, the total expected cost, which is a combined retrofit and expected travel cost, is generally higher with a higher α. The retrofit cost contributes roughly 14.6%- 20% to the total expected cost.

We are also interested in understanding the managerial insights on the integration of risk assessment into a traditional risk-neutral two-stage SP model. Table 3 compares the results of our mean-risk model with the counterparts of the two-stage SP model (first row in the table). It provides some interesting insights. First, the total expected costs of mean-risk models are equal or only trivially larger than the result of two-stage SP model even when there is a discernible increase in retrofit cost. It means that the mean-risk model can hedge against larger losses at a reasonable low total expected cost. Second, the lowest travel cost of \$285.338M is \$25.1M(=310.437-285.338) or 8% lower than the two-stage SP model, while it costs \$29 (=87-58) or 50% more in retrofit. This implies that reducing travel cost is costly. From a system-cost perspective, achieving the lowest network-wide travel cost may not be the most economical solution.

We also conducted comparisons between three different sizes of scenario sets for the same four bridges. The results and solution performances are represented in Tables 4 and 5. A larger scenario set corresponds to a larger problem size and because of our scenario generation mechanism, also has a larger number of high-damage scenarios. Between scenarios, CVaR value changes by a small extent in general. On the other hand, solution times (given in minutes) experience more noticeable changes, roughly doubling between scenarios. This is to be expected because the running time for each iteration of a non-parallelized decomposition algorithm is
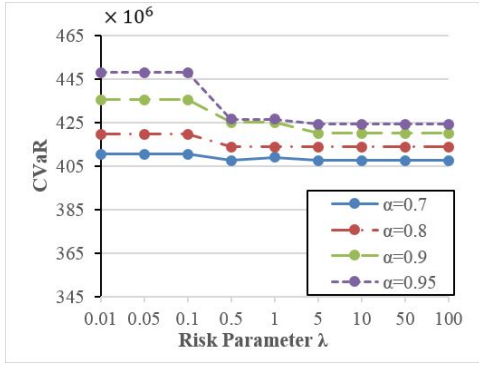
(a) $\mathbb{CVaR}_\alpha f(u)$
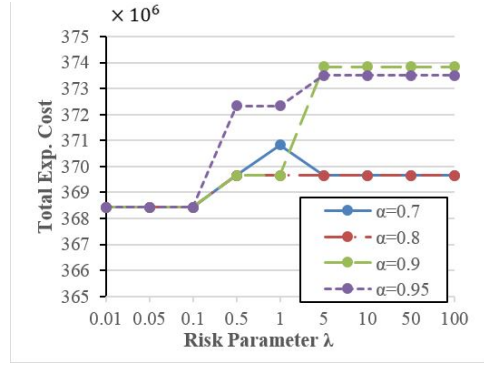
(b) Total exp. cost $\mathbb{E} f(u)$
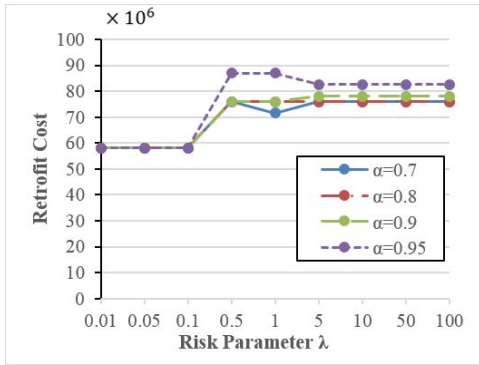
(c) Retrofit cost $b^\top u$

(d) Exp. travel cost $\mathbb{E} Q(u)$

Figure 3: Breakdown of the total cost under different combinations of risk parameters for 20 scenarios

22

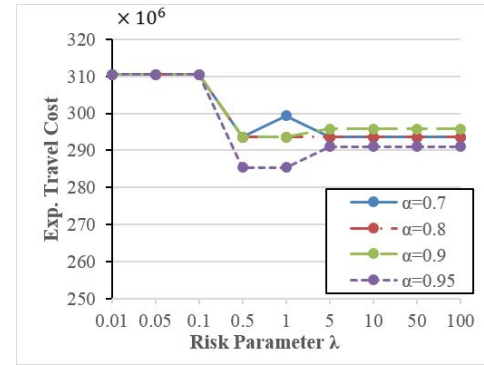Table 3: Comparisons between Risk-neutral and Mean-risk two-stage SP for 50 scenarios. The four cost columns are for total CVaR, total expected cost, retrofit cost, and expected travel cost.

λ	α	Cost ($\times 10^6$)				Retrofit Strategy			
		$\mathbb{CVaR}_\alpha f$	$\mathbb{E}f$	$b^\top u$	$\mathbb{E}Q$	A	B	C	D
0	0.7	410.502	368.437	58	310.437	3	3	2	2
	0.8	419.683	368.437	58	310.437	3	3	2	2
	0.9	435.398	368.437	58	310.437	3	3	2	2
	0.95	447.975	368.437	58	310.437	3	3	2	2
0.1	0.7	410.502	368.437	58	310.437	3	3	2	2
	0.8	419.683	368.437	58	310.437	3	3	2	2
	0.9	435.398	368.437	58	310.437	3	3	2	2
	0.95	447.975	368.437	58	310.437	3	3	2	2
0.5	0.7	407.472	369.646	76	293.646	4	3	2	2
	0.8	413.893	369.646	76	293.646	4	3	2	2
	0.9	424.954	369.646	76	293.646	4	3	2	2
	0.95	426.484	372.338	87	285.338	4	3	3	2
1	0.7	409.03	370.828	71.5	299.328	4	3	2	1
	0.8	413.893	369.646	76	293.646	4	3	2	2
	0.9	424.954	369.646	76	293.646	4	3	2	2
	0.95	426.484	372.338	87	285.338	4	3	3	2
100	0.7	407.472	369.646	76	293.646	4	3	2	2
	0.8	413.893	369.646	76	293.646	4	3	2	2
	0.9	420.096	373.841	78	295.841	4	3	3	0
	0.95	424.233	373.494	82.5	290.994	4	3	3	1

roughly proportional to the number of scenarios involved in the problem. Note that each of the 100 scenario instance takes at least 7 hours to solve within 0.5% gap, and one of them ($\lambda = 0.5, \alpha = 0.7$) takes more than 22 hours.

To test the limits of performance of our GBD method, we also experimented with 200 scenarios. On all of these instances our method had more than 20% gap after the 24 hour time limit, and because no additional insight was gained from the output, we do not include these numbers in our tables. This indicates that the current implementation of our decomposition does not scale well to 200 or more scenarios. In practice, the scenario set of a network protection problem is estimated using the intuition provided by structural engineers who are able to somewhat reasonably predict the various hazard realizations and their corresponding damage to the network. Consequently, these problems typically tend to have less than 200 scenarios. However, this may not always be true and some applications may require modeling with a large scenario set. Also, a larger number of scenarios provides a better representation of the randomness. If indeed one wishes to solve the problem with $|K| \geq 200$, either due to practical application or to have the random variables in the model be as close to having a continuous probability distribution as possible, then alternate and more efficient implementations must be sought. We offer some ideas on this in the next section. That being said, we emphasize that a decomposition approach is still preferred over solving the entire discretized problem as a MINLP; this assertion was reaffirmed by trying to solve the 200 scenario instances with a MINLP solver and observing that the solver crashed on most of them or had extremely high gaps after 24 hours.

6. Summary and future work

We formulated a mean-risk MINLP for transportation network protection (e.g., retrofitting highway bridges) hedging against extreme disasters (e.g., earthquakes) on a system level, where CVaR is considered as the risk measurement and integrated into the optimization framework. This is the first study that explicitly considers CVaR as the risk measure in the field of transportation network protection. The mean-risk formulation is a nonconvex MINLP, but we show that the recourse function can be reformulated to be convex in the bridge retrofit variables, which appear as first stage decisions. This leads to the development of a Benders-type decomposition algorithm to solve the MINLP.

We demonstrate the mean-risk model and decomposition method using two numerical examples: (i) a small nine-node network used to validate the proposed decomposition method and exhibit its superior performance in comparison to standard MINLP software; (ii) the benchmark Sioux Falls network to explore the correlations between risk parameters and retrofit decisions and their impacts on the system costs. We investigated the capacity of our solution method in handling different sized scenario sets and also compared the results of our mean-risk model with the risk-neutral model to understand the costs and effects of using a more risk-averse model. From the results, there are several worthy notes. First, by using a weighted mean-risk criterion, the mean-risk model hedges against larger losses where the two risk coefficients reflect

Table 4: Total expected and CVaR costs ($\times 10^6$) under different number of scenarios.

λ	α	$K = 20$		$K = 50$		$K = 100$	
		$\mathbb{CVaR}_\alpha f$	$\mathbb{E} f$	$\mathbb{CVaR}_\alpha f$	$\mathbb{E} f$	$\mathbb{CVaR}_\alpha f$	$\mathbb{E} f$
0	0.7	399.143	365.798	410.502	368.437	417.665	370.661
	0.8	408.018	365.798	419.683	368.437	430.958	370.661
	0.9	426.197	365.798	435.398	368.437	453.774	370.661
	0.95	438.264	365.798	447.975	368.437	482.858	370.661
0.1	0.7	399.143	365.798	410.502	368.437	417.665	370.661
	0.8	408.018	365.798	419.683	368.437	418.16	371.612
	0.9	426.197	365.798	435.398	368.437	430.395	371.612
	0.95	438.264	365.798	447.975	368.437	439.092	371.612
0.5	0.7	399.143	365.798	407.472	369.646	409.375	371.612
	0.8	408.018	365.798	413.893	369.646	418.16	371.612
	0.9	409.962	370.116	424.954	369.646	425.02	373.346
	0.95	412.771	370.116	426.484	372.338	431.136	373.346
1	0.7	399.143	365.798	409.03	370.828	408.011	373.346
	0.8	401.749	369.721	413.893	369.646	416.344	373.346
	0.9	410.505	369.721	424.954	369.646	425.461	374.152
	0.95	412.771	370.116	426.484	372.338	428.039	374.875
100	0.7	396.316	370.116	407.472	369.646	408.011	373.346
	0.8	401.749	369.721	413.893	369.646	416.55	374.152
	0.9	407.975	375.106	420.096	373.841	423.003	374.875
	0.95	410.876	375.106	424.233	373.494	428.039	374.875

Table 5: Solution performances under different number of scenarios. Gap refers to optimality gap. Times are in minutes.

λ	α	$K = 20$			$K = 50$			$K = 100$		
		% Gap	Time	# Iter.	% Gap	Time	# Iter.	% Gap	Time	# Iter.
0.00	0.7	0.10	147.68	31	0.00	342.17	30	0.00	687.05	28
	0.8	0.10	156.75	31	0.00	338.43	30	0.00	690.12	28
	0.9	0.10	152.76	31	0.00	334.37	30	0.00	684.33	28
	0.95	0.10	153.87	31	0.00	334.44	30	0.00	687.51	28
0.1	0.7	0.34	142.62	27	0.00	291.35	31	0.00	757.93	31
	0.8	0.34	148.43	28	0.00	377.1	31	0.00	738.95	30
	0.9	0.00	170.25	31	0.00	284.38	29	0.17	580.88	28
	0.95	0.00	164.37	30	0.00	350.08	30	0.00	604.62	26
0.5	0.7	0.09	160.82	29	0.01	309.52	26	0.38	1336.77	26
	0.8	0.33	152.93	29	0.33	303.3	24	0.37	579.1	26
	0.9	0.06	141.15	25	0.01	641.13	25	0.05	632.5	27
	0.95	0.00	110.53	22	0.43	225.92	24	0.07	553.78	23
1	0.7	0.32	126.02	29	0.47	246.38	27	0.07	494.85	27
	0.8	0.01	153.35	28	0.16	236.6	26	0.13	489.22	26
	0.9	0.32	84.0	21	0.44	295.07	23	0.46	530.88	23
	0.95	0.22	102.82	20	0.24	210.3	22	0.37	464.2	19
100	0.7	0.09	128.43	23	0.02	301.83	25	0.03	488.6	26
	0.8	0.01	114.7	21	0.01	301.25	25	0.19	494.52	22
	0.9	0.01	81.02	20	0.03	170.68	18	0.03	412.75	18
	0.95	0.66	92.45	20	0.19	155.65	16	0.04	401.73	17

decision makers' risk preferences. It has a slightly larger total expected cost (retrofit cost plus travel cost) than the two-stage SP model and there is a discernible increase in retrofit cost and decrease in travel cost. Second, there are quite a few duplicated solutions with different combinations of risk parameters.

Several future directions involving both the modeling and algorithmic part would be worthy research efforts. From a modeling perspective, incorporating traffic equilibrium to model route choices of network users seems relevant. This will make the model a Mathematical Program with Equilibrium Constraints (MPEC). One of the challenges would be converting this MPEC to a MINLP through regularization or penalization. Once it is in the form of MINLP, we may apply the developed decomposition method for obtaining solutions. In addition, more realistic assumptions on post-disaster traffic capacity (i.e., θ_a^k) may be included by integrating the network model with structural analysis. The structural analysis that relates the bridge performance with retrofit strategies that cost differently may produce a nonlinear bridge traffic capacity-cost relationship. Instead of assuming a constant or linear relationship as in most optimization-based transportation network protection problems, we could use finite element analysis to construct a structural performance-retrofit level relationship between the structural strength and allocated budget for each bridge. Lastly, one may also consider modeling with more general quantile risk measures and empirically comparing the solutions obtained from different risk measures.

Several enhancements can be explored on the algorithmic side to obtain a more sophisticated method that achieves faster convergence on problems with large number of scenarios. First, the subproblems can be solved in parallel at each iteration. Second, the decomposition can be implemented via a one-tree approach where a single branch-and-cut tree is maintained for the master problem and at each integer feasible node of this tree, subproblems are solved to generate globally valid optimality cuts. The choice of modeling and optimization software in this paper present a handicap with respect to these two extensions, and hence alternate implementations must be adopted. Third, alternate convex reformulations of the recourse function deserve attention. These may lead to stronger cutting planes for each scenario. Finally, this paper proposed a Benders-type (also called primal) decomposition algorithm; a natural extension would be a dual (also called scenario) decomposition algorithm which would require different convexification techniques.

Acknowledgement

References

[1] I. Buckle, I. Friedland, J. Mander, G. Martin, R. Nutt, M. Power, Seismic retrofitting manual for highway structures: Part 1–Bridges, Technical Report, US Department of Transportation, Federal Highway Administration, 2006.

[2] ASCE, 2013 Report Card for America's Infrastructure, American Society of Civil Engineers, 2013.

[3] L. Chang, F. Peng, Y. Ouyang, A. Elnashai, B. Spencer, Bridge seismic retrofit program planning to maximize postearthquake transportation network capacity, Journal of Infrastructure Systems 18 (2012) 75–88.

[4] Y. Fan, C. Liu, Solving stochastic transportation network protection problems using the progressive hedging-based method, Networks and Spatial Economics 10 (2010) 193–208.

[5] C. Liu, Y. Fan, F. Ordóñez, A two-stage stochastic programming model for transportation network protection, Computers & Operations Research 36 (2009) 1582–1590.

[6] L. J. LeBlanc, E. K. Morlok, W. P. Pierskalla, An efficient approach to solving the road network equilibrium traffic assignment problem, Transportation Research 9 (1975) 309–318.

[7] Y. Fan, C. Liu, R. Lee, A. S. Kiremidjian, Highway network retrofit under seismic hazard, Journal of Infrastructure Systems 16 (2010) 181–187.

[8] A. S. Mohaymany, N. Pirnazar, Critical routes determination for emergency transportation network aftermath earthquake, in: 2007 IEEE International Conference on Industrial Engineering and Engineering Management, IEEE, 2007, pp. 817–21.

[9] K. Viswanath, S. Peeta, Multicommodity maximal covering network design problem for planning critical routes for earthquake response, in: Transportation Research Board 82nd Annual Meeting, Transportation Research Record, National Research Council, 2003, pp. 1–10.

[10] A. Nagurney, On the relationship between supply chain and transportation network equilibria: A supernetwork equivalence with computations, Transportation Research Part E: Logistics and Transportation Review 42 (2006) 293–316.

[11] A. Nagurney, Mathematical models of transportation and networks, in: W.-B. Zhang (Ed.), Mathematical Models in Economics, volume II, Encyclopedia of Life Support Systems, 2007, pp. 346–384.

[12] M. Patriksson, The traffic assignment problem: models and methods, VSP, The Netherlands, 1994.

28

[13] S. Peeta, A. Ziliaskopoulos, Foundations of dynamic traffic assignment: The past, the present and the future, Networks and Spatial Economics 1 (2001) 233–265.

[14] Y. Sheffi, Urban Transportation Networks: Equilibrium Analysis with Mathematical Programming Methods, Prentice-Hall, Englewood Cliffs, NJ, 1985.

[15] J. R. Birge, F. Louveaux, Introduction to stochastic programming, Springer Series in Operations Research and Financial Engineering, Springer New York, second edition edition, 2011.

[16] F. Carturan, C. Pellegrino, R. Rossi, M. Gastaldi, C. Modena, An integrated procedure for management of bridge networks in seismic areas, Bulletin of Earthquake Engineering 11 (2013) 543–559.

[17] K. Rokneddin, J. Ghosh, L. Dueñas-Osorio, J. E. Padgett, Bridge retrofit prioritisation for ageing transportation networks subject to seismic hazards, Structure and Infrastructure Engineering 9 (2013) 1050–1066.

[18] K. Rokneddin, J. Ghosh, J. E. Padgett, L. D. Osorio, The effects of deteriorating bridges on bridges on the bridge network connectivity, in: Structures Congress 2011, ASCE, 2011, pp. 2993–3007.

[19] Y. Zhou, S. Banerjee, M. Shinozuka, Socio-economic effect of seismic retrofit of bridges for highway transportation networks: a pilot study, Structure and Infrastructure Engineering 6 (2010) 145–157.

[20] G. Barbarosoglu, Y. Arda, A two-stage stochastic programming framework for transportation planning in disaster response, Journal of the Operational Research Society 55 (2004) 43–53.

[21] A. Atamtürk, M. Zhang, Two-stage robust network flow and design under demand uncertainty, Operations Research 55 (2007) 662–673.

[22] H. Sun, Z. Gao, J. Long, The robust model of continuous transportation network design problem with demand uncertainty, Journal of Transportation Systems Engineering and Information Technology 11 (2011) 70–76.

[23] Y. Yin, S. M. Madanat, X.-Y. Lu, Robust improvement schemes for road networks under demand uncertainty, European Journal of Operational Research 198 (2009) 470–479.

[24] Y. Lou, Y. Yin, S. Lawphongpanich, Robust approach to discrete network designs with demand uncertainty, Transportation Research Record (2009) 86–94.

[25] F. Andersson, H. Mausser, D. Rosen, S. Uryasev, Credit risk optimization with conditional value-at-risk criterion, Mathematical Programming 89 (2001) 273–291.

[26] R. T. Rockafellar, S. Uryasev, Optimization of conditional value-at-risk, Journal of Risk 2 (2000) 21–42.

[27] S. Yau, R. H. Kwon, J. Scott Rogers, D. Wu, Financial and operational decisions in the electricity sector: contract portfolio optimization with the conditional value-at-risk criterion, International Journal of Production Economics 134 (2011) 67–77.

[28] W. Zhang, H. Rahimian, G. Bayraksan, Decomposition algorithms for risk-averse multistage stochastic programs with application to water allocation under uncertainty, INFORMS Journal on Computing 28 (2016) 385–404.

[29] E. A. V. Toso, D. Alem, Effective location models for sorting recyclables in public management, European Journal of Operational Research 234 (2014) 839–860.

[30] N. Noyan, Risk-averse two-stage stochastic programming with an application to disaster management, Computers & Operations Research 39 (2012) 541–559.

[31] C. Kwon, Conditional value-at-risk model for hazardous materials transportation, in: S. Jain, R. Creasey, J. Himmelspach, K. White, M. Fu (Eds.), Proceedings of the 2011 Winter Simulation Conference (WSC), IEEE, 2011, pp. 1708–1714.

[32] P. Artzner, F. Delbaen, J.-M. Eber, D. Heath, Coherent measures of risk, Mathematical Finance 9 (1999) 203–228.

[33] S. Ahmed, Convexity and decomposition of mean-risk stochastic programs, Mathematical Programming 106 (2006) 433–446.

[34] G. C. Pflug, Some remarks on the value-at-risk and the conditional value-at-risk, in: S. P. Uryasev (Ed.), Probabilistic Constrained Optimization: Methodology and Applications, volume 49 of *Nonconvex Optimization and its Applications*, Springer US, Boston, MA, 2000, pp. 272–281.

[35] C. I. Fábián, Handling CVaR objectives and constraints in two-stage stochastic models, European Journal of Operational Research 191 (2008) 888–911.

[36] R. Schultz, S. Tiedemann, Conditional value-at-risk in stochastic programs with mixed-integer recourse, Mathematical Programming 105 (2006) 365–386.

[37] R. Schultz, Risk aversion in two-stage stochastic integer programming, in: G. Infanger (Ed.), Stochastic Programming, volume 150 of *International Series in Operations Research & Management Science*, Springer, 2011, pp. 165–187.

[38] T. G. Cotton, L. Ntaimo, Computational study of decomposition algorithms for mean-risk stochastic linear programs, Mathematical Programming Computation 7 (2015) 471–499.

[39] C. I. Fábián, C. Wolf, A. Koberstein, L. Suhl, Risk-averse optimization in two-stage stochastic models: Computational aspects and a study, SIAM Journal on Optimization 25 (2015) 28–52.

[40] W. Ogryczak, A. Ruszczynski, Dual stochastic dominance and related mean-risk models, SIAM Journal on Optimization 13 (2002) 60–78.

[41] Y. Huang, S. Parmelee, W. Pang, Optimal retrofit scheme for highway network under seismic hazards, International Journal of Transportation Science and Technology 3 (2014) 109–128.

[42] S. Burer, A. N. Letchford, Non-convex mixed-integer nonlinear programming: a survey, Surveys in Operations Research and Management Science 17 (2012) 97–106.

[43] A. M. Geoffrion, Generalized Benders decomposition, Journal of Optimization Theory and Applications 10 (1972) 237–260.

[44] K. Mackie, B. Stojadinovic, Residual displacement and post-earthquake capacity of highway bridges, in: Proceedings of the Thirteenth World Conference on Earthquake Engineering, pp. 1–16.

[45] H. Yang, M. G. H. Bell, Models and algorithms for road network design: a review and some new developments, Transport Reviews 18 (1998) 257–278.

[46] Bureau of Public Roads, Traffic Assignment Manual, Urban Planning Division, US Department of Commerce, 1964.

[47] C. A. Floudas, Generalized Benders decomposition, in: Nonlinear and Mixed-Integer Optimization, Oxford University Press, 1995, pp. 114 – 143.

[48] A. Gupte, S. Ahmed, M. Cheon, S. Dey, Solving mixed integer bilinear problems using MILP formulations, SIAM Journal on Optimization 23 (2013) 721–744.

[49] M. Tawarmalani, N. V. Sahinidis, Global optimization of mixed-integer nonlinear programs: A theoretical and computational study, Mathematical Programming 99 (2004) 563–591.

[50] G. McCormick, Computability of global solutions to factorable nonconvex programs: Part I. convex underestimating problems, Mathematical Programming 10 (1976) 147–175.

[51] E. Balas, Disjunctive programming, Annals of Discrete Mathematics 5 (1979) 3–51.

[52] O. K. Gupta, A. Ravindran, Branch and bound experiments in convex nonlinear integer programming, Management science 31 (1985) 1533–1546.

[53] I. Quesada, I. E. Grossmann, An LP/NLP based branch and bound algorithm for convex MINLP optimization problems, Computers & chemical engineering 16 (1992) 937–947.

[54] E. M. Smith, C. C. Pantelides, A symbolic reformulation/spatial branch-and-bound algorithm for the global optimisation of nonconvex MINLPs, Computers & Chemical Engineering 23 (1999) 457–478.

[55] T. Westerlund, F. Pettersson, An extended cutting plane method for solving convex MINLP problems, Computers & Chemical Engineering 19 (1995) 131–136.

[56] R. Fletcher, S. Leyffer, Solving mixed integer nonlinear programs by outer approximation, Mathematical Programming 66 (1994) 327–349.

[57] U. Klanšek, Solving the nonlinear discrete transportation problem by MINLP optimization, Transport 29 (2014) 1–11.

[58] T. Lastusilta, M. R. Bussieck, T. Westerlund, An experimental study of the GAMS/AlphaECP MINLP solver, Industrial & Engineering Chemistry Research 48 (2009) 7337–7345.

[59] P. Bonami, L. T. Biegler, A. R. Conn, G. Cornuéjols, I. E. Grossmann, C. D. Laird, J. Lee, A. Lodi, F. Margot, N. Sawaya, et al., An algorithmic framework for convex mixed integer nonlinear programs, Discrete Optimization 5 (2008) 186–204.

[60] K. Abhishek, S. Leyffer, J. Linderoth, FilMINT: An outer approximation-based solver for convex mixed-integer nonlinear programs, INFORMS Journal on computing 22 (2010) 555–567.

[61] E. Choi, R. DesRoches, B. Nielson, Seismic fragility of typical bridges in moderate seismic zones, Engineering Structures 26 (2004) 187–199.